Electrospinning of photocrosslinked and degradable fibrous scaffolds

Andrea R. Tan,[1] Jamie L. Ifkovits,[1] Brendon M. Baker,[1,2] Darren M. Brey,[1] Robert L. Mauck,[1,2] Jason A. Burdick[1]

[1]*Department of Bioengineering, University of Pennsylvania, Philadelphia, Pennsylvania 19104*

[2]*McKay Orthopaedic Research Laboratory, Department of Orthopaedic Surgery, University of Pennsylvania, Philadelphia, Pennsylvania 19104*

Received 23 July 2007; revised 27 September 2007; accepted 22 October 2007
Published online 6 February 2008 in Wiley InterScience (www.interscience.wiley.com). DOI: 10.1002/jbm.a.31853

Abstract: Electrospun fibrous scaffolds are being developed for the engineering of numerous tissues. Advantages of electrospun scaffolds include the similarity in fiber diameter to elements of the native extracellular matrix and the ability to align fibers within the scaffold to control and direct cellular interactions and matrix deposition. To further expand the range of properties available in fibrous scaffolds, we developed a process to electrospin photocrosslinkable macromers from a library of multifunctional poly(β-amino ester)s. In this study, we utilized one macromer (A6) from this library for initial examination of fibrous scaffold formation. A carrier polymer [poly(ethylene oxide) (PEO)] was used for fiber formation because of limitations in electrospinning A6 alone. Various ratios of A6 and PEO were successfully electrospun and influenced the scaffold fiber diameter and appearance. When electrospun with a photoinitiator and exposed to light, the macromers crosslinked rapidly to high double bond conversions and fibrous scaffolds displayed higher elastic moduli compared to uncrosslinked scaffolds. When these fibers were deposited onto a rotating mandrel and crosslinked, organized fibrous scaffolds were obtained, which possessed higher moduli (~4-fold) in the fiber direction than perpendicular to the fiber direction, as well as higher moduli (~12-fold) than that of nonaligned crosslinked scaffolds. With exposure to water, a significant mass loss and a decrease in mechanical properties were observed, correlating to a rapid initial loss of PEO which reached an equilibrium after 7 days. Overall, these results present a process that allows for formation of fibrous scaffolds from a wide variety of possible photocrosslinkable macromers, increasing the diversity and range of properties achievable in fibrous scaffolds for tissue regeneration. © 2008 Wiley Periodicals, Inc. J Biomed Mater Res 87A: 1034–1043, 2008

Key words: polymers; biodegradable; fibrous scaffolds; electrospinning; poly(β-amino esters)

INTRODUCTION

Electrospun biodegradable scaffolds are a useful tool for the engineering of numerous tissues, particularly those of the musculoskeletal system.[1] To fabricate such scaffolds, suspended droplets of a polymer melt solution are electrically charged until charge repulsion overcomes the surface tension of the droplet and a stable polymer jet is formed. As the jet elongates and solvent evaporates, an ultrathin polymer strand is formed and collected onto a grounded surface.[2] The fibers within the resulting scaffold more closely mimic the size and structure of the native extracellular matrix than other previously investigated scaffolds, which can lead to beneficial cellular interactions.[3] Additionally, collection methodologies used in forming such scaffolds can be varied.[4,5] For example, a rotating collection mandrel can be deployed to generate scaffolds with a high degree of fiber alignment. These structures may then serve as 3D micropatterns whose architecture mimics that of many fiber-reinforced tissues.[6–9]

These nano- and micro-scale fibrous scaffolds have many applications for tissue engineering. Our own long-term goal is to use such scaffolds for the repair of fiber-reinforced tissues of the musculoskeletal system. These tissues, including tendon, ligament, the annulus fibrosus region of the intervertebral disc, and the knee meniscus, all function to transmit the high mechanical forces that arise with locomotion. Hallmarks of these dense fibrous tissues include a high collagen content organized along a prevailing fiber

Correspondence to: J. A. Burdick; e-mail: burdick2@seas.upenn.edu

Contract grant sponsors: University of Pennsylvania University Research Foundation, Merck Undergraduate Research Scholarship (ART), Ashton Fellowship (JLI), Department of Education GAANN Fellowship (BMB)

© 2008 Wiley Periodicals, Inc.

direction that is generally coincident with the principal loading direction. This characteristic enables tissue function, which is significantly diminished following injury and the formation of disorganized scar tissue. Taking the meniscus as an example, there are ~1,500,000 arthroscopic surgical procedures of the knee performed annually, and of these, more than half are related to the meniscus fibrocartilage of the knee.[10] Injury to, or loss of, the meniscus inhibits efficient load transfer in the knee and precipitates long-term joint changes, including osteoarthritis. Current treatments for meniscus damage (including partial or total meniscectomy) treat acute symptoms such as pain and joint locking,[11,12] but do not restore function to the knee. We have recently reported on the fabrication of engineered meniscus constructs using a fiber-aligned electrospun scaffolding system, and have shown that the scaffold architecture can promote functional maturation of constructs.[7]

A number of biodegradable polymers, such as poly(α-hydroxy esters)[13,14] and polyurethanes,[15] as well as natural polymers, such as collagen[16–18] and silk fibroin,[16–20] have been electrospun into scaffolds for use in tissue regeneration applications. Each starting polymer possesses unique mechanical and degradation properties, allowing for a range of scaffold properties to be obtained. By carefully selecting the polymer, one can control the initial mechanical properties and degradation kinetics of the electrospun scaffold.[14] For example, a recent study by Li et al. showed that the electrospinning of six different poly(α-hydroxy esters) resulted in scaffolds whose mechanics and degradation depended on the choice of polymer for scaffold fabrication.[14] While existing polymers show promise, it may be useful to further expand the available polymers used for electrospinning fibrous scaffolds to optimize cellular interactions, bulk properties, and ultimately tissue regeneration.

To this end, we have recently synthesized a large library of photopolymerizable and degradable macromers based on poly(β-amino esters) (PBAEs).[21] Photocrosslinkable PBAE macromers are easily synthesized with no byproducts, and macromer constituents are inexpensive and commercially available. When formed as films, members of this library show a wide range of physical properties (mechanics and degradation), spanning at least two orders of magnitude.[21] Furthermore, it was recently shown that simple alterations in PBAE molecular weight can lead to dramatic changes in polymer mechanics, degradation, and cellular interactions.[22] Such a range of properties in this library may be useful in the optimization of fibrous scaffold properties toward tissue regeneration applications.

The overall aim of this study was therefore to assess the feasibility of electrospinning photocrosslinkable macromers, using a candidate from the novel PBAE library as an example. There are no current techniques for the electrospinning of low molecular weight photocrosslinkable polymers, and thus, the novelty to this work is the development of new processing technology. Specifically, one macromer from the library was selected based on its favorable bulk properties (e.g., slow degradation and viable cellular interactions) and was electrospun into fibrous scaffolds. The formed scaffolds were characterized with respect to reaction behavior, mass loss, and degradation products, and both initial mechanical properties and those with degradation. An in-depth analysis of these scaffolds toward the regeneration of a specific tissue is beyond the scope of this report, yet this study represents a significant advance in the design of fibrous scaffolds for tissue regeneration since a wide range of radically crosslinked and biodegradable polymers can now be electrospun using this process. Importantly, these results show the feasibility of electrospinning photocrosslinkable macromers and provide a foundation for further optimization of engineered fibrous tissues.

MATERIALS AND METHODS

Macromer synthesis and selection

PBAEs were synthesized by the conjugate addition of primary amines to diacrylates by mixing the liquid precursors and reacting overnight at 90°C with stirring.[21] For the synthesis of macromer A6, diethylene glycol diacrylate (A, Scientific Polymer Products) was mixed with isobutylamine (6, Sigma) in a 1.2:1 molar ratio. This notation coincides with our initial report on the PBAE library. The A6 molecular weight was confirmed using ^{1}H NMR (Bruker Advance 360 MHz, Bruker, Billerica, MA). Polymer films were made by first adding the photoinitiator 2-dimethoxy-2-phenyl acetophenone (DMPA, Ciba-Geigy) to the macromer by dissolving DMPA in methylene chloride, mixing with the macromer, and evaporating off the methylene chloride in a dessicator. The macromer/DMPA solution was injected between two glass slides with a 1-mm spacer and polymerized with exposure to ultraviolet light (Blak Ray, ~10 mW/cm^2) for 10 min. For initial studies, 1-cm-diameter discs were punched from the slabs and degraded in phosphate-buffered saline (PBS) at 37°C and the mass loss was recorded over 12 weeks.

For cellular interaction studies, films were prepared on the bottom of tissue culture plates as previously described.[22] Briefly, the macromer/initiator solution was dissolved in ethanol at a 1:2 (w/v) ratio and polymerized in 24-well plates under nitrogen purge with ultraviolet light for 10 min. Films were sterilized with exposure to a germicidal lamp in a laminar flow hood for 30 min and then treated with PBS and media prior to cell seeding. Bovine mesenchymal stem cells (MSCs) were isolated from the tibial trabecular bone marrow of 3–6-month-old calves and expanded as described in Ref. 23. MSCs were seeded on the films at a density of 50,000 cells/well in DMEM

supplemented with 10% fetal bovine serum and 1× penicillin/streptomycin/fungizone and cultured for either 24 h or 7 days. At these time points, cells were fixed in formalin-free fixative (Accustain, Sigma) for 25 min. The cells were permeabilized with 0.25% Triton X-100 in PBS for 10 min, and nonspecific binding sites were blocked with 3% bovine serum albumin and 0.1% Tween-20 in PBS for 15 min at 37°C. The fixed cells were stained for actin with TRITC-conjugated phalloidin (1 μg/mL in PBS, Sigma, St. Louis, MO) for 30 min at room temperature. The nuclei were then stained with DAPI (1:2500, Sigma) for 5 min at room temperature. Films were rinsed three times with PBS between each of the previous steps and images were taken on a fluorescent microscope (Axiovert, Zeiss, Germany) with a digital camera (Axiovision, Zeiss). The total cell number was determined by counting nuclei in at least five random fields on five individual films for each composition at each time point. The area of the field was determined using a Bright-Line hemacytometer.

Electrospinning of nanofibrous scaffolds and characterization

For electrospinning, macromer A6 was dissolved in 90% EtOH to obtain a final macromer concentration of 50% (w/v). DMPA was then added to attain a final DMPA solution of 0.5 wt % of the mass of macromer. Poly(ethylene oxide) (PEO, 200 kDa) was introduced as a carrier polymer to facilitate fiber formation during electrospinning. A 10% (w/v) solution of PEO was produced by dissolution in 90% EtOH, and the PEO and A6 solutions were mixed at various ratios. Electrospinning was carried out using a custom apparatus consisting of a metal spinneret through which the polymer solution is expressed, a high voltage power supply, and a grounded collecting surface.[9] Spinnerets were 18-gauge blunt-ended needles and the solution flow rate was governed by gravimetric pressure. Solutions were electrospun at 13 kV over 20 cm and collected for 90 min on a stationary plate (for SEM and FTIR analysis) or for 12 h on a rotating mandrel at ~10 m/s (for mass loss and tensile testing). Nonaligned mats were also fabricated by spinning onto a stationary plate for 12 h (for tensile testing). The scaffolds ranged in thickness from ~0.6 to 1.4 mm, depending on alignment and position on the mandrel.

Scaffolds were analyzed with scanning electron microscopy (SEM, JEOL 6400, Penn Regional Nanotechnology Facility) before and after polymerization (365 nm wavelength, ~5 mW/cm^2). Fiber diameter was quantified using the length measurement tool in ImageJ (v1.38, NIH). One hundred measurements were taken for each SEM image for the different PEO:A6 ratios. Double bond conversion within fibrous scaffolds was monitored with ultraviolet light exposure using Attenuated Total Internal Reflectance-Fourier Transform Infrared Spectroscopy (ATR-FTIR, Nicolet 6700, Thermo Fisher Scientific, Waltham, MA) and real-time monitoring of the acrylate peak (~1630 cm^{-1}).

Mechanical properties and mass loss

Rectangular samples (5 × 25 mm^2) were excised as strips from electrospun sheets for mechanical testing. Uniaxial tensile testing was performed on both untreated scaffolds (uncrosslinked) and after sheets were crosslinked with ultraviolet light. Samples were taken from both nonaligned and aligned sheets, and tested parallel and perpendicular to the prevailing fiber direction. Additionally, aligned samples were incubated in water for 1, 3, or 6 days, dried by lyophilization, and mechanically tested. Dried constructs were preconditioned with 10 sinusoidal cycles of 0.5% strain at 0.1 Hz and subsequently tested to failure at a constant strain rate of 0.1%/s using a 5848 Microtester equipped with a 50-N load cell (Instron, Canton, MA). The tensile modulus of the construct was calculated from the linear region of the stress–strain curve (0–3%) and initial sample geometry.

Five-millimeter-diameter punches were excised and mass loss was determined after incubation in deionized water at 37°C for 6 h and subsequently at daily intervals over the period of a week. The fiber morphology was also monitored throughout the period of mass loss. The soluble fraction of the bulk polymer was determined by immersing the punches in methylene chloride overnight to allow unreacted macromer to swell from the network. After drying, the soluble fraction was calculated as a percentage of initial mass loss and repeated daily until the daily incremental mass loss was negligible.

Additionally, ^{1}H NMR was used to investigate the eluted products after incubation in deionized water. The supernatant at each mass loss time point was collected, lyophilized, and prepared for ^{1}H NMR analysis by dissolving each sample in deuterated chloroform. A 65:35 PEO:A6 sample was also prepared for analysis. Each sample was scanned and processing was completed using SpinWorks (University of Manitoba, Canada). Values are reported as a ratio of the amount of PEO to A6 at the mass loss time point to the ratio of the amount of PEO to A6 in the initial electrospun solution.

Statistical analysis

Anova with Tukey's *post hoc* test was used to determine significant difference among groups, with $p < 0.05$. All values are reported as the mean ± the standard deviation.

RESULTS

Macromer synthesis and characterization

One macromer, termed A6, was selected from the PBAE library and synthesized by the step-growth polymerization of the amine and diacrylate [Fig. 1(A)]. End group analysis of the ^{1}H NMR spectra was used to determine the number average molecular weight of A6 to be 1.34 kDa. After synthesis, macromer A6 was crosslinked into networks using a free-radical photoinitiated polymerization. A6 was identified as a potential candidate for tissue engineering applications because of its degradation profile and favorable cellular interactions. The degradation profile shows gradual mass loss over 3 months

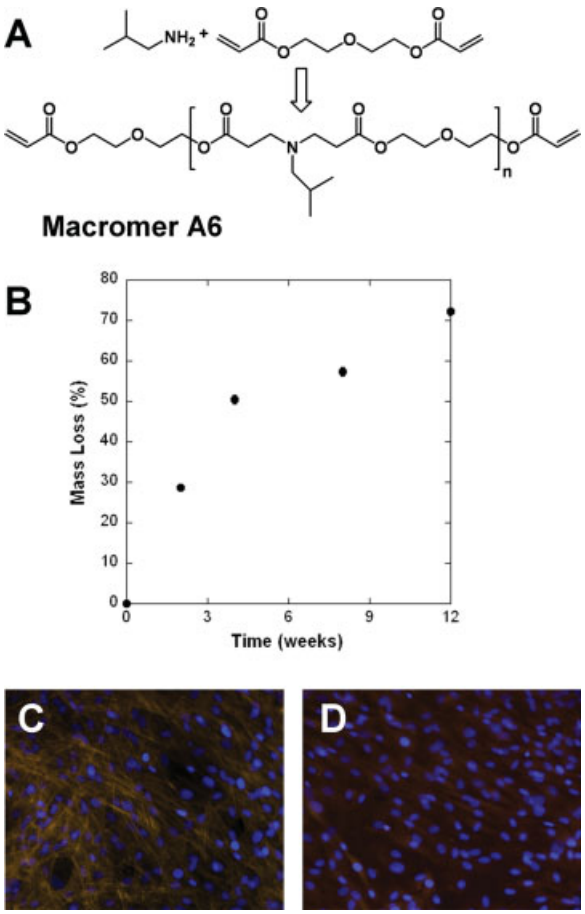

Figure 1. A: Synthesis scheme and structure of macromer A6 used for electrospinning. B: Mass loss behavior for networks formed from A6 in slab form ($n = 3$). Bovine mesenchymal stem cell adhesion to films of networks formed from macromer A6 (C) and control tissue culture polystyrene (D) after 7 days. [Color figure can be viewed in the online issue, which is available at www.interscience.wiley.com.]

[Fig. 1(B)] and is indicative of a bulk degrading polymer. Although this does not span complete degradation, placement of networks in strong base leads to complete degradation (data not shown).

The interaction of MSCs with films of A6 and a control of tissue culture polystyrene (TCPS) was assessed and showed comparable adhesion after both 24 h and 7 days. For instance, cell adhesion on networks fabricated from A6 was ~98% and ~80% the numbers of cells on TCPS, after 24 h and 7 days, respectively. The interaction of MSCs with the films was also assessed by actin and nuclear staining [Fig. 1(C,D)]. After 7 days, a near confluent monolayer of cells was observed on both surfaces with actin fibers more pronounced in MSCs cultured on A6 than on TCPS.

Fibrous scaffold fabrication

Because of the desirable initial properties of A6 (i.e., slow degradation, cytocompatibility), this macromer was selected for electrospinning. However, initial attempts to spin A6 alone resulted in electrospraying, whereby beads were formed, likely due to the low molecular weight of A6. Thus, a process was developed in which A6 was electrospun with a high molecular weight carrier polymer (i.e., PEO). A schematic of the electrospinning process is shown in Figure 2, where a polymer solution (A6, PEO, and initiator in ethanol) is placed in a spinneret and a voltage is applied. The polymer is collected either on a grounded metal sheet or a rotating shaft, exposed to ultraviolet light for crosslinking, and then exposed to water for subsequent PEO removal.

SEM images of electrospun fibrous scaffolds at a variety of PEO:A6 ratios are shown in Figure 3(A). Distinct fibers are seen with morphological changes as the A6 content is increased. Specifically, the fiber diameter increased and more welding is found at fiber–fiber junctions with decreasing PEO content. Fiber diameter increased significantly for A6 contents greater than 20% [$p < 0.05$, Fig. 3(B)]. From these initial SEM characterizations, the 65:35 PEO:A6 ratio was selected based on its ability to maintain fiber form and limit junction formation, while limiting PEO content.

Reaction characterization

After formation, the crosslinking of the selected 65:35 PEO:A6 scaffold with ultraviolet light was monitored through the disappearance of the reactive acrylate peak with time using ATR-FTIR [Fig. 4(A)]. Through these measurements, the double bond conversion was quantified as a function of polymeriza-

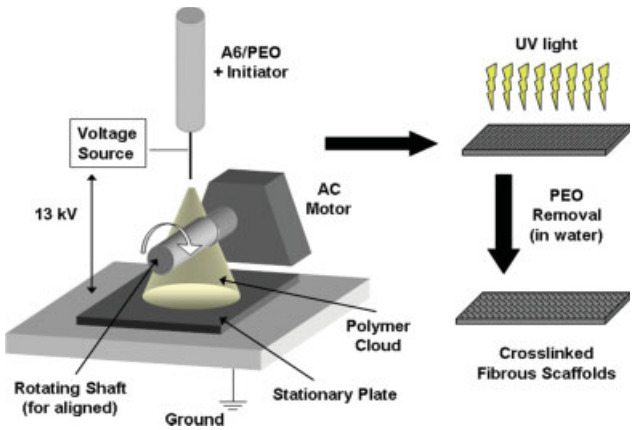

Figure 2. Schematic of the electrospinning process. A solution of the macromer, PEO, and photoinitiator in 90% ethanol is placed in the spinneret to form a fibrous mat of the macromer and PEO. This mat is then exposed to ultraviolet light for crosslinking and then water for partial removal of PEO. [Color figure can be viewed in the online issue, which is available at www.interscience.wiley.com.]

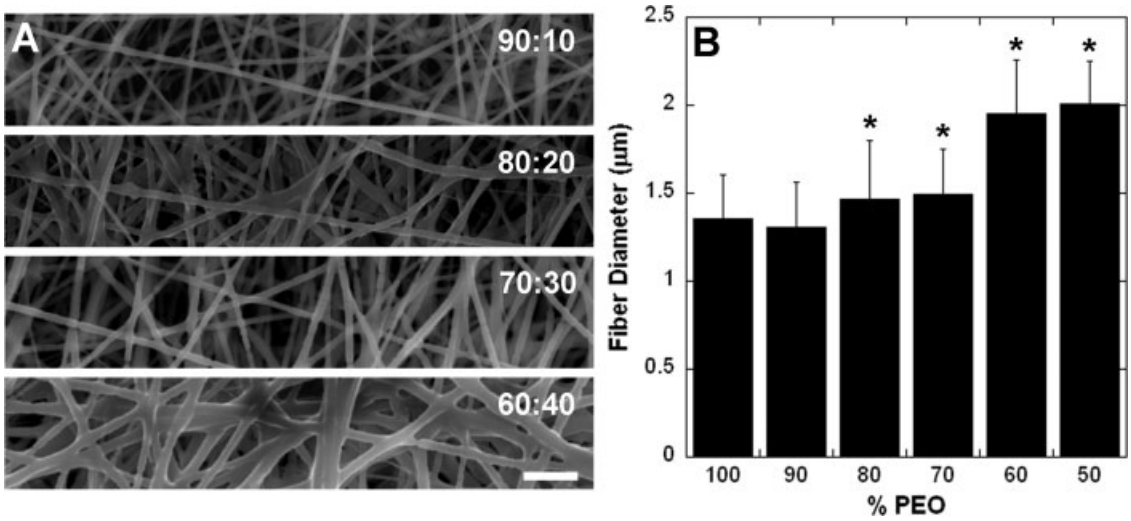

Figure 3. Morphology of electrospun fibers. A: Electrospun fibers of PEO and macromer A6 at various mass ratios (PEO:A6); scale bar = 10 μm. B: Fiber diameter as a function of PEO concentration. *$p < 0.05$ compared to 100% PEO fibers.

tion time [Fig. 4(B)]. Maximal conversion was reached after ~8 min and was high (>95%), indicating successful crosslinking. The structural integrity of the scaffold was assessed visually and by placing the scaffold in methylene chloride to dissolve away unreacted components. SEM images showed no changes in fiber structure with crosslinking, and failure of the samples to dissolve in methylene chloride demonstrated uniformity in sample integrity with depth.

Mechanical properties

Mechanical properties of formed scaffolds were determined before and after crosslinking using a uniaxial tensile test to failure. Results from mechanical testing illustrated that crosslinked samples had a higher tensile modulus than their uncrosslinked counterparts ($p < 0.001$). Specifically, for crosslinked scaffolds, a modulus of ~1.3, ~23, and ~12 MPa [Fig. 5(A)] was determined in nonaligned and aligned samples tested in the fiber direction, and aligned samples tested perpendicular to the fiber direction samples, respectively. For comparison, uncrosslinked scaffolds had a modulus of ~0.3, ~6, and ~1.1 MPa for these same conditions. Additionally, aligned scaffolds exhibited a mechanical anisotropy ratio (parallel/perpendicular properties) of 5.45 before crosslinking and 1.91 after crosslinking, indicating structural and mechanical differences dependent on directional orientation. Crosslinked, aligned fibrous scaffolds tested in the parallel direction also exhibited significantly higher tensile moduli compared to bulk A6 polymer slabs, crosslinked nona-

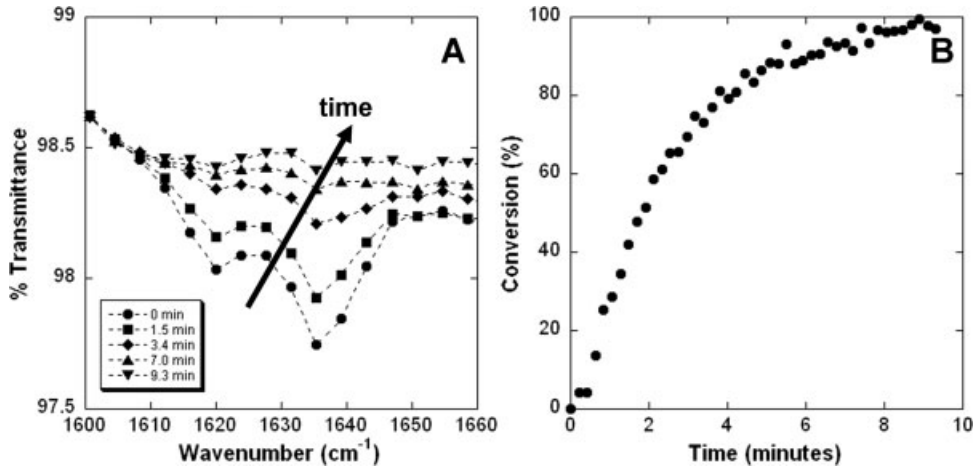

Figure 4. Photopolymerization of fibrous scaffolds. A: Decrease in the acrylate peak with exposure to light. B: Double bond conversion with time.

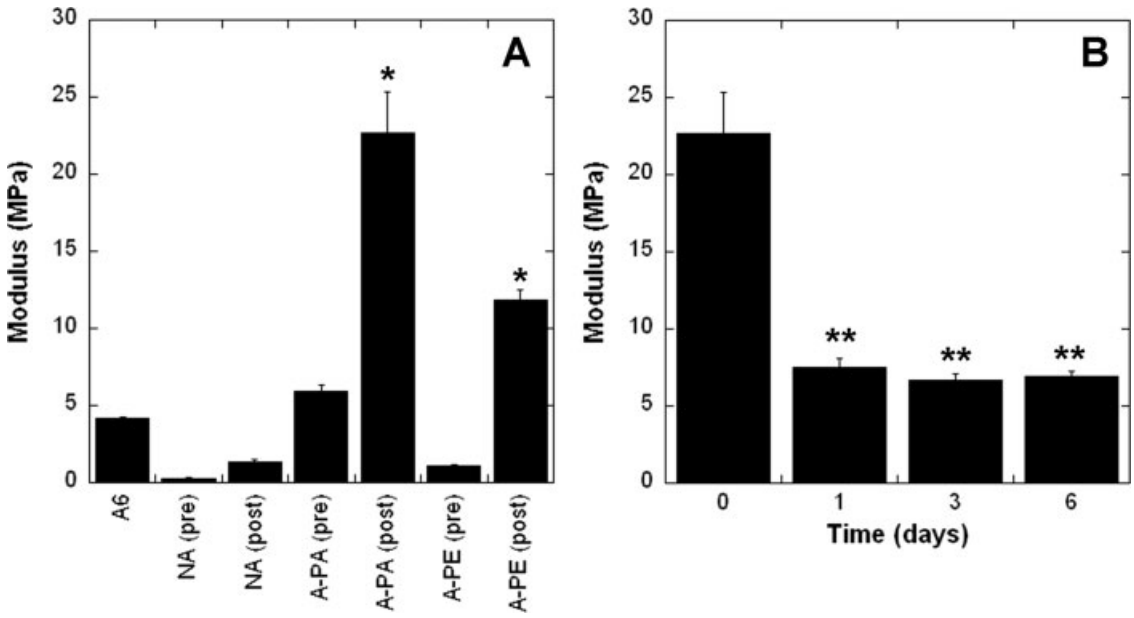

Figure 5. Mechanical properties of electrospun scaffolds. A: Modulus for A6 slab (without PEO) and both nonaligned (NA) and aligned (A) scaffolds before (pre) and after (post) crosslinking tested both parallel (PA) and perpendicular (PE) to fiber alignment ($n = 6$). B: Scaffold modulus (A-PA, post) initially and after incubation in water for 1, 3, and 6 days ($n = 6$). *$p < 0.05$ compared to uncrosslinked scaffold of same orientation and **$p < 0.05$ compared to samples before incubation in water.

ligned scaffolds, and crosslinked aligned scaffolds tested in the perpendicular direction ($p < 0.001$). It is expected that the fibrous scaffolds would have a higher moduli than the A6 slabs because they contain a second polymer component (PEO), which can contribute to the polymer mechanics. Additionally, there is potential for polymer chains to align within a fiber during electrospinning, which could influence mechanics, but would not occur in the polymer slabs. With exposure to an aqueous environment for 1, 3, and 6 days, scaffolds exhibited significantly lower tensile moduli when compared with initial constructs [~7.5, ~6.6, ~6.9 MPa, respectively; $p < 0.001$; Fig. 5(B)] as PEO eluted from the fibrous structures.

Mass loss and NMR characterization

Sample degradation was further analyzed with submersion in an aqueous environment and monitoring of the mass loss and NMR analysis of degradation products. The mass loss observed for the crosslinked samples after submersion in water included a very rapid loss of mass within the first 6 h, followed by a more gradual release for the next 5 days, and then a plateau [Fig. 6(A)]. Long-term degradation analysis was not performed on these samples. SEM analysis of the fibrous scaffolds after mass loss indicates some swelling and welding of the fiber junctions [Fig. 6(B)]. NMR analysis of the initial 35:65 A6:PEO solution spectrum identified peaks at 4.2 and 3.6 ppm, which can be attributed to A6 and an overlap of A6 and PEO, respectively [Fig. 7(A)]. These peaks were analyzed in the supernatants of the mass loss samples and a representative spectrum is shown in Figure 7(B). Both visual analysis (decrease in peak from A6 compared to peak from PEO) and quantification (Fig. 7, inset) indicate that the primary component being released from the fibrous scaffolds after submersion in water is PEO. For instance, there is more than seven times as much PEO in the release solution after 6 h compared to A6 than in the initial solutions prepared for electrospinning. This ratio decreases with continued exposure, as the scaffold approaches a plateau in this initial mass loss regime.

DISCUSSION

Current tissue engineering regenerative solutions that utilize electrospinning are limited to the properties offered by previously electrospun polymers. In this study, we address the need to increase the number of polymers that can be electrospun by introducing photocrosslinkable PBAE macromers from a library of polymers with a wide range of properties.[21] The objective of this work was to develop an electrospinning process that could be used to form fibrous scaffolds from a wide range of photocrosslinkable precursors. Photocrosslinked networks are finding application for the engineering of numerous tissues.[24,25] Only minimal work has been performed

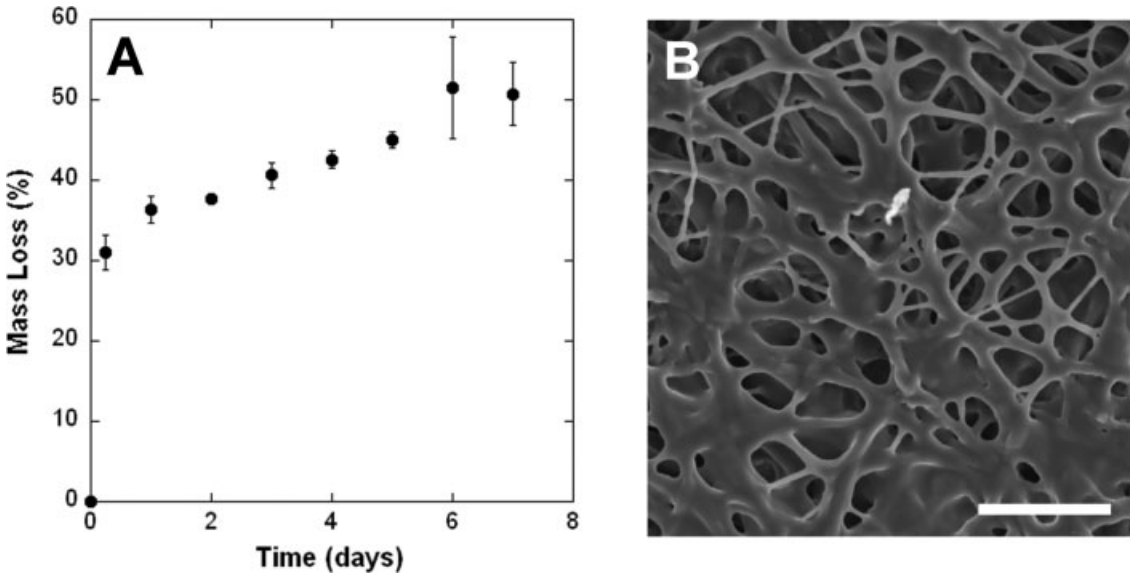

Figure 6. Mass loss for electrospun and crosslinked fibers. A: Mass loss with incubation in water for up to a week (n = 3 per time point). B: SEM image of scaffold 4 days after incubation in water; scale bar = 25 μm.

on the electrospinning of methacrylated or acrylated precursors and these have been primarily directed toward the production of swollen hydrogels and coatings,[26,27] not stable scaffolds with sufficient mechanical integrity for use in three-dimensional tissue engineering applications. For this initial study, we selected one macromer with potential properties of interest for tissue regeneration scaffolds. Macromer A6 was selected through a screening process that illustrated that networks formed from the macromer exhibited a gradual hydrolytic degradation profile and enabled positive cellular interactions comparable to a control of TCPS. While the macromer A6 is promising for tissue engineering applications, the objective of this work was primarily to develop a procedure for the electrospinning of radically polymerizable macromers in general, and not to identify this specific chemistry as optimal for tissue engineering. In the future, this technology can be implemented to electrospin any candidate from the PBAE library at different molecular weights to tune fibrous scaffold properties for specific applications.

The first step in this process was the identification of a method to electrospin low molecular weight macromers. Typically, high molecular weight polymers are chosen because of their desired molecular interactions and inherent viscosity during the spinning process. After macromer A6 failed to form fibers in initial experiments, it was coelectrospun along with a high molecular weight polymer, PEO. Coelectrospinning of blended polymers has been previously employed to exploit beneficial features of the individual components.[28] In this study, PEO was chosen for this purpose as it is readily electrospun, will assist in fiber formation, will not interact with

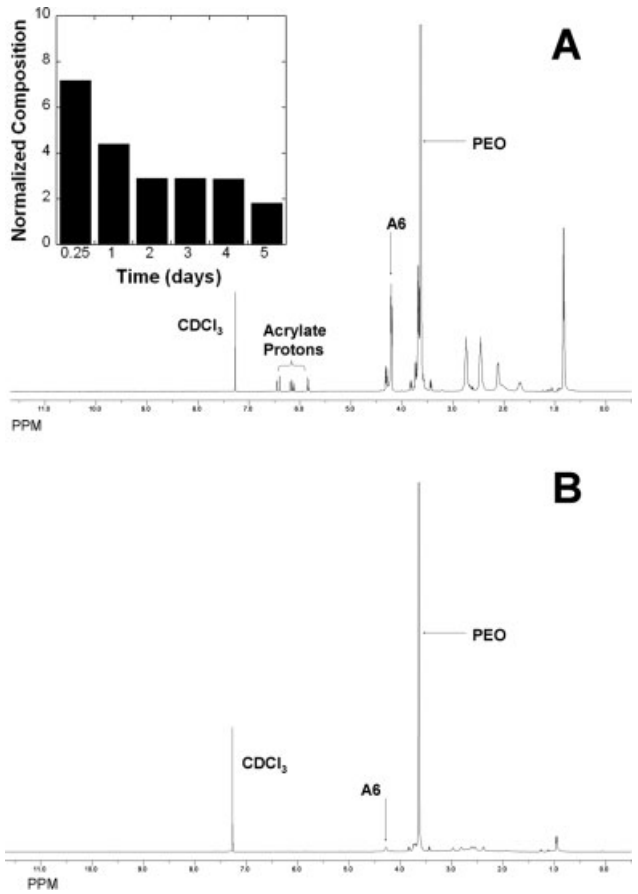

Figure 7. NMR spectrum of the initial electrospun solution of A6 and PEO (A) and a representative spectrum of the released products after 6 h (B). Inset: Normalized composition of the released products compared to the initial electrospun sample. These results indicate that the majority of the mass loss initially is from released PEO and a small amount of A6.

the PBAE macromer during crosslinking, and will then elute from the crosslinked network rapidly with submersion in an aqueous environment. The macromer was successfully electrospun and formed fibrous scaffolds, with morphological changes apparent in the scaffold depending on the ratio of the photocrosslinkable macromer and carrier polymer. Specifically, the fiber diameter and junction welding increased with more macromer. The change in fiber diameter could also be influenced by the viscosity of the electrospun solution which changes with the addition of the PEO component.

One composition (65:35 PEO:A6) was chosen for subsequent analysis based on morphological features and to minimize the PEO content. When exposed to light, crosslinked networks formed, as evidenced by the decrease in the acrylate peak, an increase in scaffold modulus, and a resistance to dissolution after ultraviolet light exposure. The reaction behavior led to very high conversions, which indicates a low concentration of unreacted macromers that can elute from the crosslinked structure. While not tested specifically in this work, we speculate that the increases in mechanical properties of the formed scaffolds after exposure to ultraviolet light results from the formation of both intra- and inter-strand covalent crosslinks. Increases in interstrand physical linkages (or bonding), via variations in solvent formulation, has previously been shown to increase the mechanical properties of scaffolds composed of segmented polyurethane.[29]

The mechanical strength of both nonaligned and aligned scaffolds formed from this A6-PEO blend before and after covalent crosslinking, as well as the mass loss profile of these constructs and the corresponding effect on mechanical properties was determined. As reported by numerous other authors,[6,7,9,30] deposition of electrospun polymers onto a rotating mandrel produces physical alignment of the fibers with significant mechanical anisotropy. In this manuscript, we show for the first time the ability of a member of the PBAE library to be spun in this same manner.[31] Interestingly, and unlike previous reports,[9,30] the aligned scaffolds were found to have greater moduli than nonaligned scaffolds when tested in either the fiber or crossfiber directions. The morphology of the fibers may explain this finding as the aligned scaffolds appear to have an increased number of interfiber contacts (with fibers sometimes tracking along one another for significant lengths). If interfiber crosslinks form upon ultraviolet light exposure, this lengthy contact region would lead to more crosslinking between fibers in the aligned scaffolds over the nonaligned scaffolds with their more dispersed fiber junctions. Additionally, this could lead to direction-dependent differences in mechanics pre- and post-crosslinking in aligned scaffolds, which was observed with the decrease in mechanical anisotropy with ultraviolet light exposure. In this work, an ~10-fold increase in modulus is seen in the perpendicular direction with crosslinking, whereas only a 3–4-fold increase is noted in the parallel direction, where PEO and fiber alignment already dominated the mechanics.

In our degradation studies, both mass loss and mechanical testing indicate that polymer is being released from the fibrous scaffolds after immersion in water. ^{1}H NMR analysis indicates that this is primarily the PEO component, with a small amount of A6, which may be attributed to a small soluble fraction or short-term degradation. The rapid decrease in mechanics indicates that the carrier polymer provides the scaffold with a significant portion of its initial mechanical properties, and that the crosslinked A6 macromer defines the properties after mass loss has plateaued. Also, the mass loss results (<65%) indicate that not all of the PEO has been eluted within the first week. Although some cell adhesion is evident on the scaffolds (results not shown), it is limited and in clusters, which may be indicative that PEO is blocking protein adsorption, and consequently, cellular adhesion. This finding may be advantageous, as adhesion can be tailored by the introduction of adhesive peptides into the PBAE network to promote specificity in cellular interactions.[32] This will be explored when these scaffolds are developed toward a specific application.

As fibrous scaffolds are being electrospun and designed for specific tissues, the diversity of polymer properties available is essential. For instance, the mechanical properties of the substrate may dictate cellular behavior and construct integrity until complete tissue maturation. Furthermore, a range of mechanical parameters may be required for specific physiologic scenarios. For example, in the meniscus, *in vivo* strain magnitudes in the circumferential direction with normal use range between 3 and 6%.[33] Therefore, for regenerative strategies involving this tissue, scaffolds must be extensible through this range while not undergoing plastic deformation under physiologic load magnitudes. Replicating the nonlinearity of the stress–strain response and failure characteristics of biologic tissues may likewise be important. In this study, our A6 fibrous scaffolds showed a relatively linear stress–strain response, and failed abruptly at extension levels greater than 5%. Also, there were significant changes in mechanics and morphology with degradation and loss of the PEO component, which necessitates further development of specific formulations toward intended applications. For example, the fiber mechanics can be altered by choosing a different candidate from the PBAE library. Additionally, investigators have electrospun fibrous scaffolds from multiple individual polymers using separate spinnerets,[34,35] which can also lead to interesting and con-

trolled composite scaffold properties. Thus, the ability to tune these properties in individual polymer scaffolds and optimally combine them using a wide range of photocrosslinkable polymers will be essential in the next generation of functional tissue engineering of fibrous tissues.

CONCLUSIONS

In this study, fibrous scaffolds were successfully electrospun from a PBAE macromer with potential application in tissue engineering using PEO as a carrier polymer. When exposed to ultraviolet light in the presence of a photoinitiator, crosslinked networks were formed with almost 100% conversion of the double bonds and a corresponding increase in mechanical strength. Both nonaligned and aligned fibrous meshes can be formed from this process. When exposed to water, the scaffolds decrease in mass and mechanics, due primarily to release of the carrier polymer. The ability to electrospin photocrosslinkable and low molecular weight macromers will allow for the production of fibrous scaffolds with a wide range of degradation and mechanical properties, particularly from the PBAE library. This will further expand the application of fibrous scaffolds to a wider range of tissue engineering approaches.

References

1. Li WJ, Mauck RL, Tuan RS. Electrospun nanofibrous scaffolds: Production, characterization, and applications for tissue engineering and drug delivery. J Biomed Nanotech 2005;1:259–275.
2. Norman JJ, Desai TA. Methods for fabrication of nanoscale topography for tissue engineering scaffolds. Ann Biomed Eng 2006;34:89–101.
3. Li WJ, Jiang YJ, Tuan RS. Chondrocyte phenotype in engineered fibrous matrix is regulated by fiber size. Tissue Eng 2006;12:1775–1785.
4. Li D, Xia YN. Electrospinning of nanofibers: Reinventing the wheel? Adv Mater 2004;16:1151–1170.
5. Teo WE, Ramakrishna S. A review on electrospinning design and nanofibre assemblies. Nanotechnology 2006;17:R89–R106.
6. Ayres C, Bowlin GL, Henderson SC, Taylor L, Shultz J, Alexander J, Telemeco TA, Simpson DG. Modulation of anisotropy in electrospun tissue-engineering scaffolds: Analysis of fiber alignment by the fast Fourier transform. Biomaterials 2006;27:5524–5534.
7. Baker BM, Mauck RL. The effect of nanofiber alignment on the maturation of engineered meniscus constructs. Biomaterials 2007;28:1967–1977.
8. Courtney T, Sacks MS, Stankus J, Guan J, Wagner WR. Design and analysis of tissue engineering scaffolds that mimic soft tissue mechanical anisotropy. Biomaterials 2006;27:3631–3638.
9. Li WJ, Mauck RL, Cooper JA, Yuan X, Tuan RS. Engineering controllable anisotropy in electrospun biodegradable nanofibrous scaffolds for musculoskeletal tissue engineering. J Biomech 2007;40:1686–1693.
10. Rodkey WG, Steadman JR, Li ST. A clinical study of collagen meniscus implants to restore the injured meniscus. Clin Orthop Relat Res 1999;S281–S292.
11. Kang SW, Son SM, Lee JS, Lee ES, Lee KY, Park SG, Park JH, Kim BS. Regeneration of whole meniscus using meniscal cells and polymer scaffolds in a rabbit total meniscectomy model. J Biomed Mater Res A 2006;78:659–671.
12. Koski JA, Ibarra C, Rodeo SA, Warren RF. Meniscal injury and repair—Clinical status. Orthop Clin North Am 2000;31:419–436.
13. Boland ED, Telemeco TA, Simpson DG, Wnek GE, Bowlin GL. Utilizing acid pretreatment and electrospinning to improve biocompatibility of poly(glycolic acid) for tissue engineering. J Biomed Mater Res B Appl Biomater 2004;71:144–152.
14. Li WJ, Cooper JA Jr, Mauck RL, Tuan RS. Fabrication and characterization of six electrospun poly(alpha-hydroxy ester)-based fibrous scaffolds for tissue engineering applications. Acta Biomater 2006;2:377–385.
15. Khil MS, Cha DI, Kim HY, Kim IS, Bhattarai N. Electrospun nanofibrous polyurethane membrane as wound dressing. J Biomed Mater Res B Appl Biomater 2003;67:675–679.
16. Buttafoco L, Kolkman NG, Engbers-Buijtenhuijs P, Poot AA, Dijkstra PJ, Vermes I, Feijen J. Electrospinning of collagen and elastin for tissue engineering applications. Biomaterials 2006;27:724–734.
17. Matthews JA, Wnek GE, Simpson DG, Bowlin GL. Electrospinning of collagen nanofibers. Biomacromolecules 2002;3:232–238.
18. Rho KS, Jeong L, Lee G, Seo BM, Park YJ, Hong SD, Roh S, Cho JJ, Park WH, Min BM. Electrospinning of collagen nanofibers: Effects on the behavior of normal human keratinocytes and early-stage wound healing. Biomaterials 2006;27:1452–1461.
19. Min BM, Jeong L, Nam YS, Kim JM, Kim JY, Park WH. Formation of silk fibroin matrices with different texture and its cellular response to normal human keratinocytes. Int J Biol Macromol 2004;34:281–288.
20. Min BM, Lee G, Kim SH, Nam YS, Lee TS, Park WH. Electrospinning of silk fibroin nanofibers and its effect on the adhesion and spreading of normal human keratinocytes and fibroblasts in vitro. Biomaterials 2004;25:1289–1297.
21. Anderson DG, Tweedie CA, Hossain N, Navarro SM, Brey DM, Van Vliet KJ, Langer R, Burdick JA. A combinatorial library of photocrosslinkable and degradable materials. Adv Mater 2006;18:2614–2618.
22. Brey DM, Erickson IE, Burdick JA. Influence of macromer molecular weight and chemistry on poly(β-amino ester) network properties and initial cell interactions. J Biomed Mater Res. Forthcoming.
23. Mauck RL, Yuan X, Tuan RS. Chondrogenic differentiation and functional maturation of bovine mesenchymal stem cells in long-term agarose culture. Osteoarthritis Cartilage 2006;14:179–189.
24. Chung C, Mesa J, Randolph MA, Yaremchuk M, Burdick JA. Influence of gel properties on neocartilage formation by auricular chondrocytes photoencapsulated in hyaluronic acid networks. J Biomed Mater Res A 2006;77:518–525.
25. Ifkovits J, Burdick J. Review: Photopolymerizable and degradable biomaterials for tissue engineering applications. Tissue Eng 2007;10:2369–2385.
26. Kim SH, Nair S, Moore E. Reactive electrospinning of crosslinked poly(2-hydroxyethyl methacrylate) nanofibers and elastic properties of individual hydrogel nanofibers in aqueous solutions. Macromolecules 2005;38:3719–3723.
27. Pornsopone V, Supaphol P, Rangkupan R, Tantayanon S. Electrospinning of methacrylate-based copolymers: Effects of

solution concentration and applied electrical potential on morphological appearance of as-spun fibers. Polym Eng Sci 2005;45:1073–1080.
28. Dalton PD, Klinkhammer K, Salber J, Klee D, Moller M. Direct in vitro electrospinning with polymer melts. Biomacromolecules 2006;7:686–690.
29. Kidoaki S, Kwon IK, Matsuda T. Mesoscopic spatial designs of nano- and microfiber meshes for tissue-engineering matrix and scaffold based on newly devised multilayering and mixing electrospinning techniques. Biomaterials 2005;26:37–46.
30. Nerurkar N, Elliott D, Mauck R. Mechanics of oriented electrospun nanofibrous scaffolds for annulus fibrosis tissue engineering. J Orthop Res 2007;25:1018–1028.
31. Nerurkar N, Baker B, Chen C, Elliott DM, Mauck RL. Engineering of fiber-reinforced tissue with anisotropic biodegradable nanofibrous scaffolds. Conf Proc IEEE Eng Med Biol Soc 2006;1:787–790.
32. Burdick JA, Anseth KS. Photoencapsulation of osteoblasts in injectable RGD-modified PEG hydrogels for bone tissue engineering. Biomaterials 2002;23:4315–4323.
33. Jones RS, Keene GC, Learmonth DJ, Bickerstaff D, Nawana NS, Costi JJ, Pearcy MJ. Direct measurement of hoop strains in the intact and torn human medial meniscus. Clin Biomech (Bristol, Avon) 1996;11:295–300.
34. Ding B, Kimura E, Sato T, Fujita S, Shiratori S. Fabrication of blend biodegradable nanofibrous nonwoven mats via multi-jet electrospinning. Polymer 2004;45:1895–1902.
35. Madhugiri S, Dalton A, Gutierrez J, Ferraris JP, Balkus KJ Jr. Electrospun meh-ppv/sba-15 composite nanofibers using a dual syringe method. J Am Chem Soc 2003;125:14531–14538.

All in-text references underlined in blue are linked to publications on ResearchGate, letting you access and read them immediately.